Cortical and Subcortical Anatomy of the Orbitofrontal Cortex: A White Matter Microfiberdissection Study and Case Series

Philip Rauch, MD [*‡]
Carlo Serra, MD [*]
Luca Regli, MD [*]
Andreas Gruber, MD [‡]
Martin Aichholzer, MD [‡]
Harald Stefanits, MD, PhD [‡]
Paulo Abdo do Seixo Kadri, MD, PhD [§]
Lazar Tosic, MD [*]
Matthias Gmeiner, MD, PhD [‡]
Uğur Türe, MD [¶]
Niklaus Krayenbühl, MD [*]

*Department of Neurosurgery, Clinical Neuroscience Center, University Hospital, University of Zurich, Zurich, Switzerland; ‡Department of Neurosurgery, Kepler University Hospital, Johannes Kepler University, Linz, Austria; §Division of Neurosurgery, School of Medicine, Federal University of Mato Grosso do Sul, Campo Grande, Brazil; ¶Department of Neurosurgery, Yeditepe University School of Medicine, Istanbul, Turkey

Correspondence:
Carlo Serra, MD,
Department of Neurosurgery,
Clinical Neuroscience Center,
University Hospital Zürich,
Frauenklinikstrasse 10,
8091 Zurich, Switzerland.
Email: carlo.serra@usz.ch

Received, December 3, 2020.
Accepted, May 3, 2021.
Published Online, July 9, 2021.

BACKGROUND: The literature on white matter anatomy underlying the human orbitofrontal cortex (OFC) is scarce in spite of its relevance for glioma surgery.
OBJECTIVE: To describe the anatomy of the OFC and of the underlying white matter fiber anatomy, with a particular focus on the surgical structures relevant for a safe and efficient orbitofrontal glioma resection. Based on anatomical and radiological data, the secondary objective was to describe the growth pattern of OFC gliomas.
METHODS: The study was performed on 10 brain specimens prepared according to Klingler's protocol and dissected using the fiber microdissection technique modified according to U.T., under the microscope at high magnification.
RESULTS: A detailed stratigraphy of the OFC was performed, from the cortex up to the frontal horn of the lateral ventricle. The interposed neural structures are described together with relevant neighboring topographic areas and nuclei. Combining anatomical and radiological data, it appears that the anatomical boundaries delimiting and guiding the macroscopical growth of OFC gliomas are as follows: the corpus callosum superiorly, the external capsule laterally, the basal forebrain and lentiform nucleus posteriorly, and the gyrus rectus medially. Thus, OFC gliomas seem to grow ventriculopetally, avoiding the laterally located neocortex.
CONCLUSION: The findings in our study supplement available anatomical knowledge of the OFC, providing reliable landmarks for a precise topographical diagnosis of OFC lesions and for perioperative orientation. The relationships between deep anatomic structures and glioma formations described in this study are relevant for surgery in this highly interconnected area.

KEY WORDS: Glioblastoma, Glioma, Glioma growth pattern, Orbital pole, Orbitofrontal, Tumor dynamics, White matter dissection

Operative Neurosurgery 21:197–206, 2021 https://doi.org/10.1093/ons/opab243

The orbitofrontal cortex (OFC) is an architectonically heterogeneous cortical area topographically corresponding to most of the orbital surface of the frontal lobe.[1] From a physiological point of view, it seems to be implicated in several neurocognitive processes. The region, initially considered to be noneloquent, generally attracted little scientific attention until the famous brain injury of Phineas Gage influenced the perception of organic psychological disorders in the 19th century.[2] Together with the anterior insula and temporopolar cortex, Mesulam et al[22] considered the region of the OFC as part of the paralimbic belt. Nowadays, it is considered to be a multifunctional hub: it receives multiple extrinsic autonomic, sensory, olfactory, gustatory, and visual afferents, and is linked to behavioral traits such as task value and decision-making.[3,4]

Empirical evidence shows that gliomas preferentially originate in specific areas of the brain and frequently affect the frontal lobe or the OFC.[5-7] They commonly present with neuropsychological deficits because of a distortion of the elaborately arranged white matter tracts that compose its subcortical anatomy.[8-11] Detailed anatomical descriptions in humans, especially

ABBREVIATIONS: APS, anterior perforate substance; **I-L,** limen insulae; **OFC,** orbitofrontal cortex; **SI,** innominate substance

from a neurosurgical standpoint, remain however scarce. Thus, the aim of this study is to describe the surface of the OFC together with the underlying white matter anatomy. Based on anatomical findings, we describe the observed OFC glioma growth pattern in a provided prospective case series.

METHODS

Microdissection

The topographic anatomy of the OFC was studied in 10 brain specimens (10 left, 10 right hemispheres), which were obtained in routine autopsies and dissected by P.R. and C.S. between July and December 2019. The fresh specimens were prepared following Klingler's protocol and dissected via a modified white matters microdissection technique according to U.T. under high magnification.[12,13] Important surgical as well as anatomical landmarks were described in a similar fashion after meticulous study of the available macro- and microscopic literature,[1,14-17] thereby minimizing possible dissection artifacts. The anatomy of every dissection step was photographed (Nikon D 7000 camera, Sigma 105 mm f2.8/macro).

Illustrative Cases

We reviewed prospectively collected clinical and imaging data of all patients operated on a supratentorial intraparenchymal tumor located in the OFC at the University Clinic Zurich, Switzerland, between 2009 and 2017. Inclusion criteria comprised (i) >18 yr of age at the time of diagnosis, (ii) availability of at least 1 preoperative cerebral magnetic resonance imaging (MRI) study with a minimum field strength of 1.5 Tesla, and (iii) histologically verified glioma located in the OFC. Ethics board approval was obtained prior to data acquisition from the local ethics committee (KEK-2016-00 957). All patients or their legal representatives gave their written informed consent.

RESULTS

Dissection of the Inferior Aspects of the OFC

The basal surface of the frontal lobe is bordered by the medial frontal gyrus medially, by the gyrus paraterminalis and gyrus subcallosus posteromedially, and the striae olfactoriae posteriorly. It is then variably continuous with the inferior, middle, and superior frontal gyri anteriorly and laterally. The anatomical borders of the OFC itself are composed of the following structures: the frontomarginal sulcus (anterior), the olfactory sulcus (medial), and the fronto-orbital sulcus (lateral). The paleocortical olfactory trigone (ie, the medial and lateral olfactory stria, and the olfactory tubercle) completes the posterior border (Figure 1). The posterior portion of the medial orbital gyrus and the medial portion of the posterior orbital gyrus conjoin to form the orbital pole or posteromedial orbital lobule (Figures 1B, 1C, and 2A), which further extends into the transverse gyrus of the insula. Just posterior to the olfactory trigone lies the anterior perforate substance (APS), whereas the limen insulae (I-L) can be found postero-laterally to the OFC. Macroscopically, the OFC is composed of 4 gyri (ie, medial, anterior, posterior, and lateral orbital gyrus) that are delineated by the orbital sulcus or "cruciform sulcus of Rolandus."[18] The sulci are typically arranged in the shape of an "H," "K," or "X," but can be further augmented by supplementary sulci such as the intermediate and posterior sulcus or the so-called sulcus fragmentosus.[19]

Dissection is performed in a strictly step wise fashion along a caudo-rostral direction. In the first step (Figure 2B), the cortex of the OFC is removed with suction and a wooden spatula to expose the white matter superficial layer of "U-fibers" below. The temporal pole is sharply dissected along the entorhinal sulcus as to expose the APS, which is variably concealed beneath. This pentagonally shaped structure lies just posterior to the olfactory striae and is limited by the I-L laterally and the interhemispheric fissure medially, as well as the optic tract posteromedially and the entorhinal sulcus postero-laterally.[19,20] Laterally, after removal of the cortex overlying the I-L, the longitudinal fibers of the uncinate fascicle become visible, running from the temporal pole to the OFC. More medially, after removal of the thin white matter layer resembling the stratum zonale of the thalamus that covers the APS, the amygdaloseptal fibers (ie, diagonal band of Broca) are visualized below its anterior part. Careful microdissection further exposes the anterior amygdaloseptal fibers, followed by the more posterior ventral amygdalohypothalamic fibers (Figure 2B and 2C). Interspersed within these transversely running fibers are islets of grey matter corresponding to the Nucleus Basalis of Meynert (formerly considered part of the innominate substance [SI]). Just above the APS lies the so-called basal forebrain, an anatomical term that subsumes telencephalic and diencephalic structures of subpallial origin and includes the SI, the septal area, the nucleus accumbens, and the amygdala, which provides a major cholinergic input to more caudal structures.[16] Further dissection unveils, laterally, the C-shaped angle point of the uncinate fascicle at the I-L and demonstrates the fan-like projections running beneath the superficial layer of the U-fibers in the OFC. Uncinate fascicle – and inferior fronto-occipital fascicle – fibers display a parallel course at the point of the I-L and OFC with no clear distinction from one another at this level. Medially, after removal of the gyrus rectus and its underlying U-fibers, the basal extension of the forceps minor of the corpus callosum is visible running deeper than the fibers of the external capsule (Figure 2D). Medially, after decortication of the interhemispheric portion of the gyrus rectus and the medial frontal gyrus up to and including the cingulate pole, the entire inferior portion of the genu corpus callosum is exposed. Removal of the olfactory tubercle together with the SI and associated white matter tracts (diagonal band of Broca and ventral amygdalohypothalamic fibers) unveils the nucleus accumbens. Deep to the optic tract, the ventral amygdalohypothalamic fibers and the fibers of the extracapsular thalamic peduncle can be appreciated, which run just anterior to the cerebral peduncle. Between the optic tract caudally and lentiform nucleus cranially, the ansa peduncularis can be depicted, which includes amygdalohypothalamic fibers as well as thalamocortical and corticothalamic fibers of the inferior thalamic peduncle.

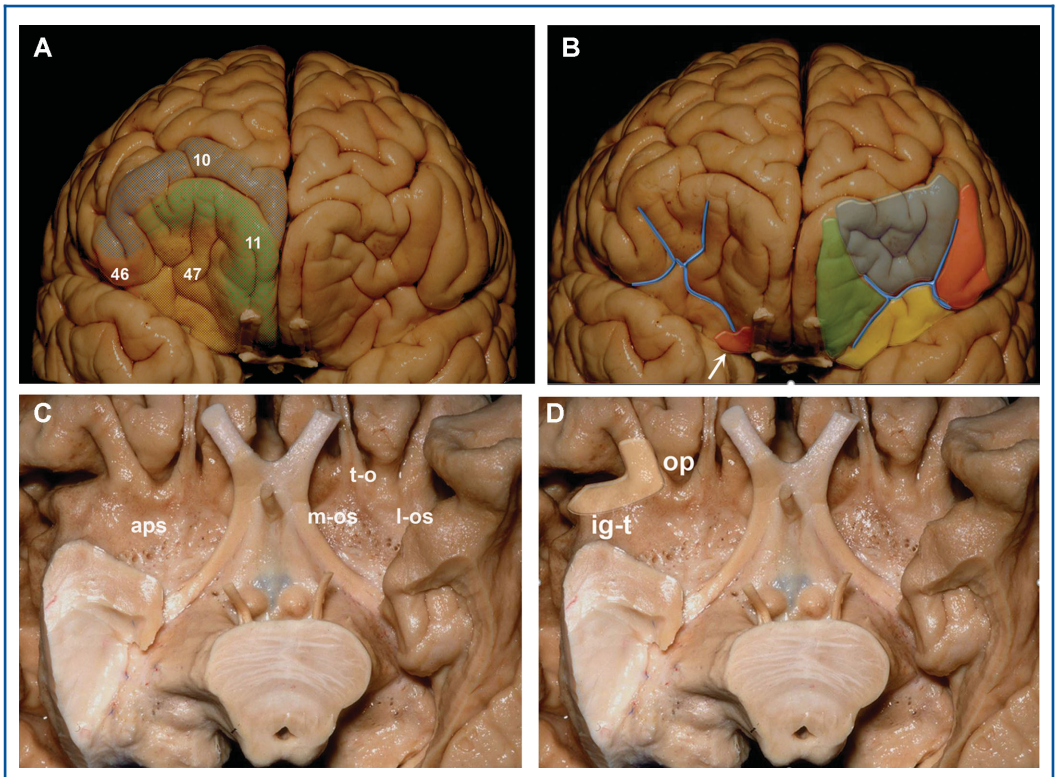

FIGURE 1. *Antero-inferior view of the frontal and temporal lobes. Brodmann areas are highlighted and numbered* **A**. *The 4 orbitofrontal gyri (anterior, medial, lateral, and posterior) are separated by the cruciform sulcus of Rolandus* **B** *(blue). The junction of the posterior medial orbital gyrus and the medial posterior orbital gyrus is also referred to as orbital pole and continues into the transverse gyrus of the insula* **B** *(white arrow). In an inferior view* **C**, *the posterior border structures of the OFC are highlighted. The APS lies just posterior to the olfactory trigone. The extension of the orbital pole into the transverse gyrus of the anterior insula is distinctly colored as visual aid* **D**. *APS, anterior perforate substance; L-OS, lateral olfactory stria; M-OS, medial olfactory stria; T-O, olfactory tubercle; OP, orbital pole; IG-T, transverse gyrus of the insula.*

As a final step (Figure 2E), the nucleus accumbens and the posteriorly located diagonal band of Broca, as well as the extracapsular thalamic peduncle are removed. In this way, the accumbofrontal fascicle is revealed beneath the fibers of the anterior commissure. The removal of the accumbofrontal fascicle and the anterior commissure eventually exposes the fibers of cerebral peduncle of the midbrain (or crus cerebri) posteriorly, which can be followed craniomedially into the anterior limb of the internal capsule. More posteriorly, the lentiform nucleus (putamen and globus pallidus) and the head of the caudate nuclei can be seen lateral and medial to the internal capsule, respectively. Anatomical structures, given their vascular relationship with the middle cerebral artery, can also facilitate a correct anatomical classification of orbitofrontal neoplasms by providing easily recognizable landmarks for radiological diagnostics (Figure 3). This pattern could be consistently found in all specimens without any relevant variation or asymmetry between the right and the left side.

Case Series

A total of 14 patients harboring a histologically verified orbitofrontal glioma were included in this study. We analyzed the preoperative MRI scans (T1, T1 + contrast, T2, Flair, and diffusion tensor imaging [DTI]) and determined the relationship of the tumor with the large bordering white matter tracts as well as the grey nucleic complexes. We observed a tumor expansion that was flanked by the white matter tracts of the forceps minor and the corpus callosum superiorly, as well as the anterior commissure postero-inferiorly. On the other hand, the grey nucleic complexes of the basal nucleic complex (including the septal region) and hypothalamus were displaced posteriorly. The external capsule limited the lateral extension of the tumor. Contrary to an isotropic tumor infiltration that would affect all surrounding structures equally, the tumors appear to grow along a path of least resistance toward the lateral ventricle posteriorly, displacing the basal forebrain (Figures 4 and 5).

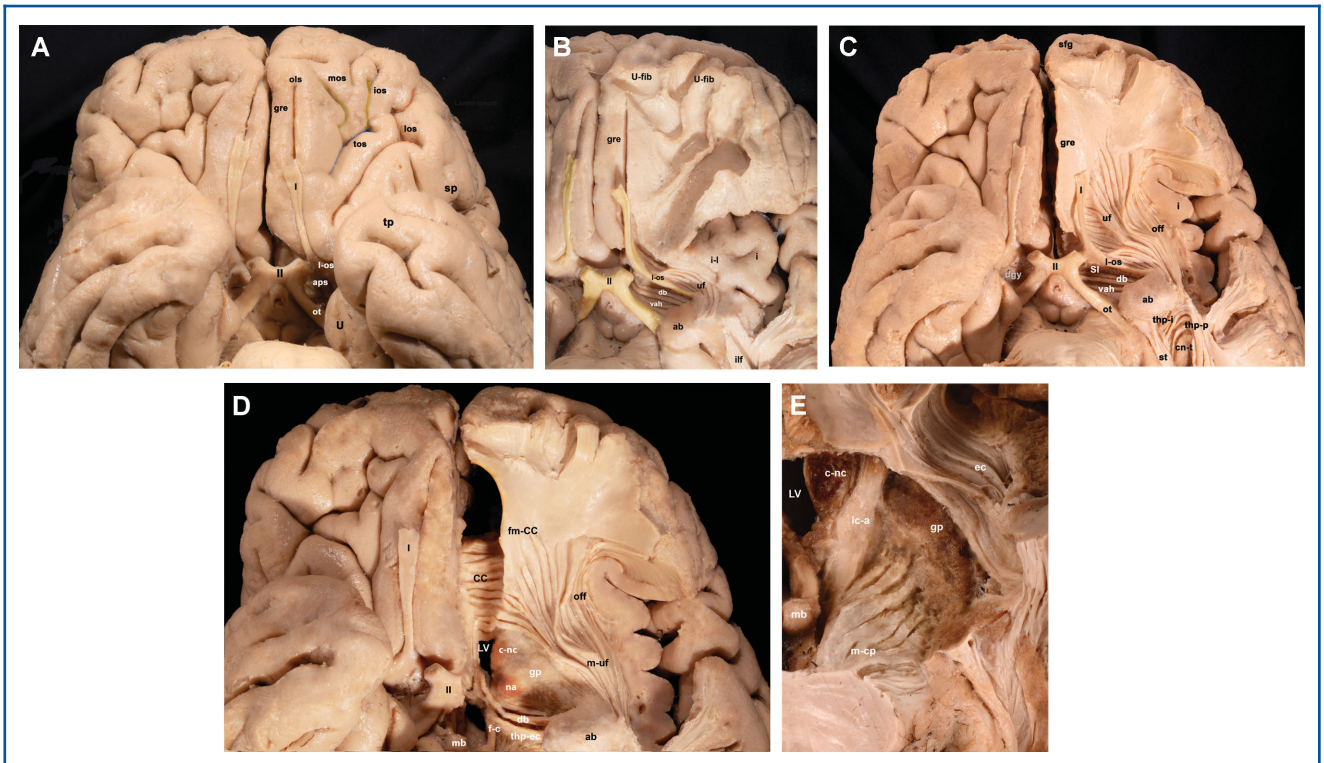

FIGURE 2. *Photographs of brain specimens showing serial dissections in an inferior to superior fashion of the basal aspects of the left cerebral hemisphere.* **A**, *Antero-inferior view after the removal of vessels and arachnoid. The sulcal anatomy of the OFC lateral to the gyrus rectus is highlighted in color.* **B**, *The temporal pole and OFC is sharply removed to expose the I-L and the "U-fibers" of the OFC. Removal of the surface layers of the APS reveals the transversely running fibers of the diagonal band of Broca and ventral amygdalohypothalamic fibers. The uncinate fascicle and lateral olfactory stria mark the posterolateral border of the orbitofrontal neocortex.* **C**, *Dissection of the "U-fibers" shows the anterolateral projections of the uncinate fascicle and inferior-fronto-occipital fascicle. After removal of the parahippocampal gyrus, the tail of the caudate nucleus, the stria terminalis, and the temporal loop of the posterior thalamic peduncle are visualized.* **D**, *Removal of the left optic chiasm, tractus opticus, lateral olfactory stria, olfactory nerve, and central uncinate fascicle reveals the lentiform nucleus and head of the caudate. Further dissection of the interhemispheric cortex of the gyrus rectus, superior frontal gyrus, and cingulate gyrus fully exposes the commissural projections of the corpus callosum.* **E**, *Removal of the extracapsular thalamic peduncle, diagonal band of Broca, and nucleus accumbens shows the cerebral peduncle of the midbrain (crus cerebri) and the anterior limb of the internal capsule below. I, olfactory nerve; II, optic nerve; AB, amygdaloid body; APS, anterior perforated substance; CC-G, genu of corpus callosum; CN-H, head of caudate nucleus; CN-T, tail of caudate nucleus; DB, diagonal band of Broca; EC, external capsule; F-C, column of fornix; FMI, fornix minor (radiation of corpus callosum); GRE, gyrus rectus; GP, globus pallidus; I, insula; IC-A, anterior limb of the internal capsule; I-L, limen insulae; ILF, inferior longitudinal fasciculus; IOS, intermediate orbital sulcus; L-OS, lateral olfactory stria; LOS, lateral orbital sulcus; LV, lateral ventricle; MB, mamillary body; M-CP, cerebral peduncle of the midbrain; M-OS, medial olfactory stria; MOS, medial orbital sulcus; NA, nucleus accumbens; OFF, occipitofrontal fascicle; OLS, olfactory sulcus; OS, orbital sulcus; OT, optic tract; PG, parahippocampal gyrus; SI, innominate substance; SP, sylvian point; ST, stria terminalis; THP-EC, extracapsular thalamic peduncle; TO, transverse orbital sulcus; TP, temporal pole; VAH, ventral amygdalohypothalamic fibers; UF, uncinate fasciculus; U, uncus.*

In all observed cases, we could observe an analogous growth pattern. Naturally, the level of displacement of the surrounding structures was dependent on the tumor size.

DISCUSSION

In this study, we demonstrate the cortical and subcortical anatomy of the OFC via a white matter microdissection approach.

From a neurosurgical point of view, these anatomical insights are helpful for an exact topographic diagnosis of an OFC glioma, which in turn allows to choose for an appropriate surgical approach to the OFC. Thus, a lateral transcortical approach can be avoided and the frontal extension of the external capsule spared together with fibers travelling deep to the gyri of the frontal convexity. As a matter of fact, a lateral transcortical approach would disrupt not only the superficial cortex and U-fibers but also, depending on the chosen trajectory, the superior longitudinal fascicle, the external capsule, and of the corona radiate (Figures 6 and 7). Such an extensive functional disconnection is not only avoidable, but could also aggravate neurological and neuropsychological deficits. These may vary from very subtle deficits only, to language deficits or a so-called "frontal lobe syndrome."[9,21,39]

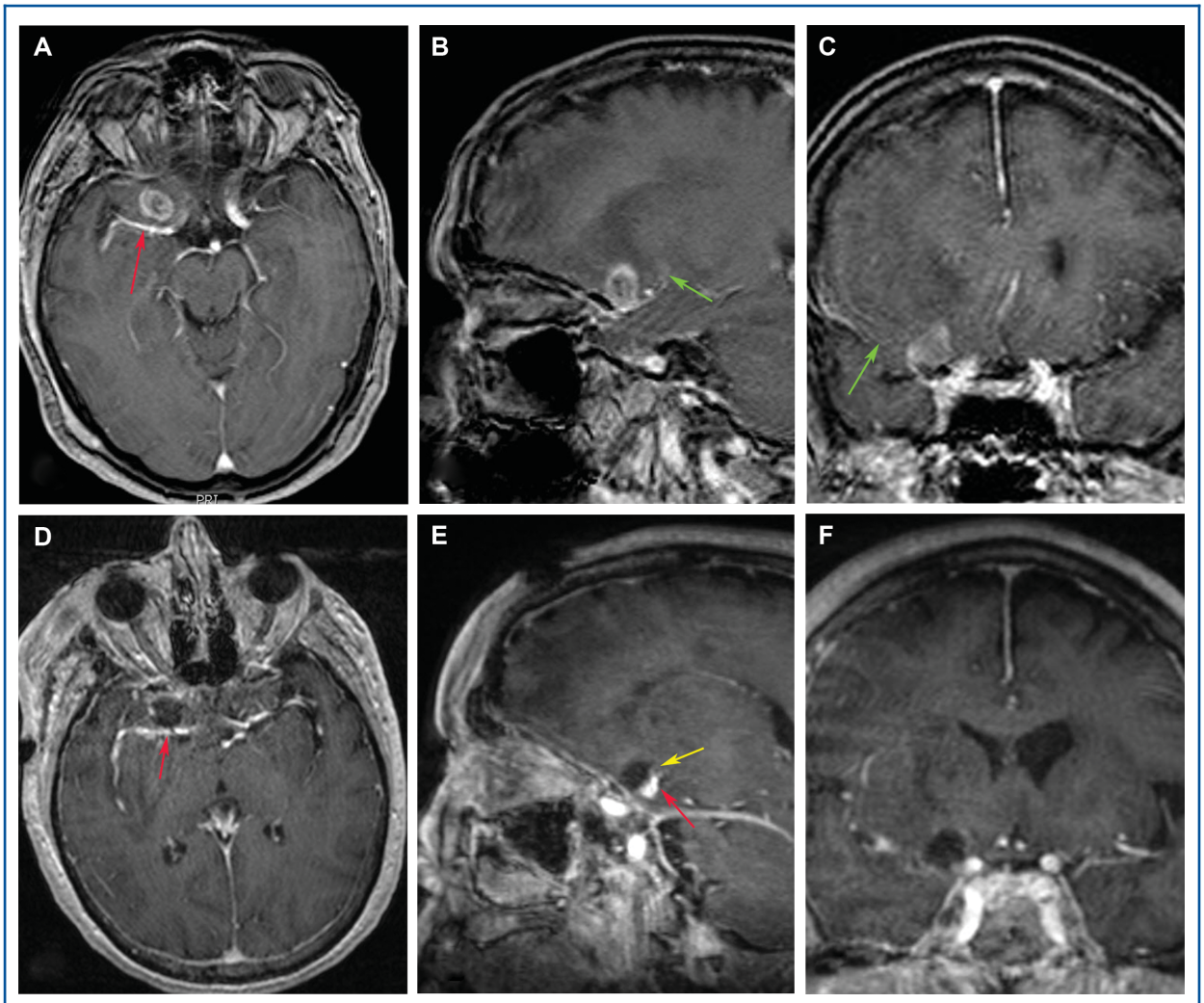

FIGURE 3. *T1 with contrast preoperative* **A-C** *(upper row) and postoperative* **D-F** *(lower row) (from left to right: transversal, sagittal, and coronal) imaging of a patient with an orbitofrontal glioblastoma. The tumor is located in the orbital pole, the junction of the medial orbital gyrus and posterior orbital gyrus* **A-C**. *A gross total resection via a pterional approach was achieved* **D-F**. *Just posterior to anatomical border of the OFC (ie, olfactory trigone), the APS and the posterolateral I-L can be found. They can be directly or indirectly recognized on MRI via surrogate anatomical structures such as the M1 segment of the internal carotid artery, just inferior to the APS. Bordering structures of the OFC are marked with an arrow: green arrow, I-L; red arrow, M1 of the middle cerebral artery; and yellow arrow, APS.*

Secondly, the topographical knowledge that we gained allows us to speculate for a glioma growth along the path of least resistance, at least on a macroscopic level. We hypothesize that bordering large white matter tracts and grey nucleic complexes can actually deter gliomas' migratory capabilities so significantly that stereotypical growth patterns can be discerned. Our fiber dissection examinations visibly demonstrate the anatomical relationship of the white and grey matter structures to the OFC from which the tumors originate. This approach indirectly highlights the anatomical limits of the described growth pattern. Furthermore, the depicted tumor pattern emphasizes the propensity of glioma cells to spread within the confines of their relative embryological compartment. This concept of selective topographical vulnerability of the brain can also be referred to as "pathoclisis."[8]

Glioma Growth Characteristics

Descriptions of macroscopic glioma behavior and the tendency toward histological compartmentalization in humans were initially provided by Filimonoff in 1947,[22] by Yakovlev in 1959,[23] and were later refined by Yasargil in 1992.[24,25] In 1938, the

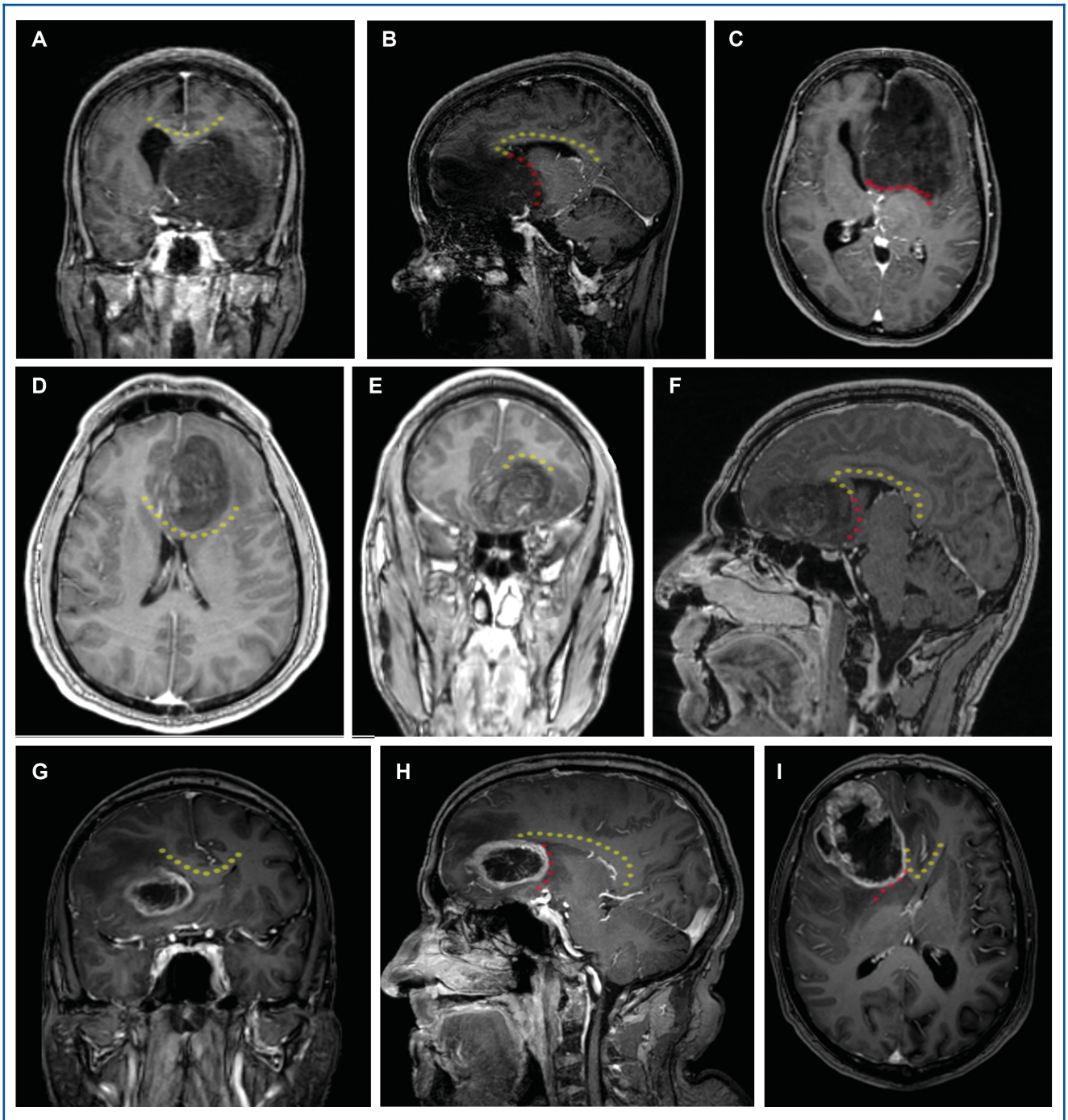

FIGURE 4. *MRI T1 with contrast: patients marked individually from (*A-C*, transversal,* D-F*, sagittal, and* G-I*, coronal views), the strongly displaced but not infiltrated corpus callosum is highlighted (yellow dotted line). Striatal and diencephalic structures appear similarly displaced, but not infiltrated (red dotted line). Cystic and diffuse gliomas reveal an analogous growth pattern directed towards the area subcallosa.*

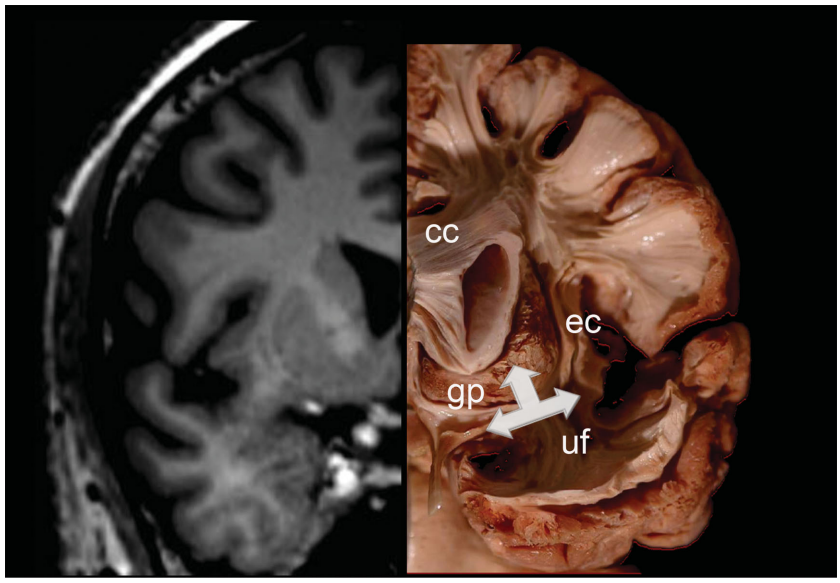

FIGURE 5. *Juxtaposition of T1 coronal MRI (left) and a 3-dimensional anatomical specimen (right) after white matter microdissection. The superior and posterolateral borders of the described tumor growth pattern are distinctly highlighted as visual aid. Grey arrow: 3-dimensional growth direction of gliomas along the path of least resistance between the highlighted structures. CC, corpus callosum; EC, external capsule; GP, globus pallidus; UF, uncinate fascicle.*

German neuropathologist Hans Joachim Scherer[26] favored the theory of expansion along the perivascular space and along myelinated axon bundles.

There has, however, been a great evolution of our conceptual understanding of the migratory capacities of glioma cells in recent years, which now includes fundamentally important aspects of microenvironmental factors and neuronal cell regulation. It was shown that spatial and temporal variations in signaling pathways can affect phenotypic and ultimately, behavioral attributes in glioma cells.[27-32] Hence, the complex genetic aberrations may lead to several different tumor subgroups and ultimately different tumor invasion patterns. In our case series, Isocitrate-Dehydrogenase mutation and 1p/19q co-deletion could however not be associated with a difference in tumor morphology and expansion pattern, most likely due to a limited sample size.

To solely reduce glioma evolution to migration along pre-existing tracks or confine its development exclusively to its embryological compartment consequentially appears to be a rather simplistic approach.

On a macroscopic level, however, there is a prominent appeal to the before-mentioned theories. Firstly, in mathematical models, a preferred migration route along large white matter tracts such as the internal capsule or corpus callosum has frequently been suggested (ie, butterfly glioma); also, computed tumor simulation models have shown increased accuracy when white matter imaging data (DTI) were employed.[33-36] Secondly, phylogenetically different areas of the brain vary in their cytoarchitectonic features of cortical layers as well as their complexity. They differ not only structurally – ie, no lamination in the oldest and most primitive areas in contrast to the most complex 6-layered structure of the neocortical areas – but also in their regional connectivity, genetic expression patterns, and transcriptional profiles.[37,38] It seems therefore reasonable that a region-specific tumor microenvironment could have an influence on glioma infiltration patterns, at least in the earlier stages of the disease. Yasargil[24] and Schramm[39] showed a propensity for glioma cells to spread within its respective phylogenetic site for mesocortical and allocortical tumors – neocortical and medial structures such as the basal ganglia were spared in all cases, but the most advanced glioblastoma formations.

The reason why grey substance areas provide a similar, if not stronger, barrier to glioma invasion than the large white matter tracts is currently under debate and has not yet been fully elucidated.

Various methods have been used to study glioma invasion and cancer cell distribution, ie, in organotypic brain slice cultures, in Vivo in animal models, or in silico or in Vitro cultures.[40-42] Although these techniques have provided a detailed insight into the specific characteristics of glioma evolution, they typically fail to authentically represent the complexity and heterogeneity of human brain tissue sufficiently. Thus, the systematic macroscopic and anatomy specific description of glioma behavior in real-life

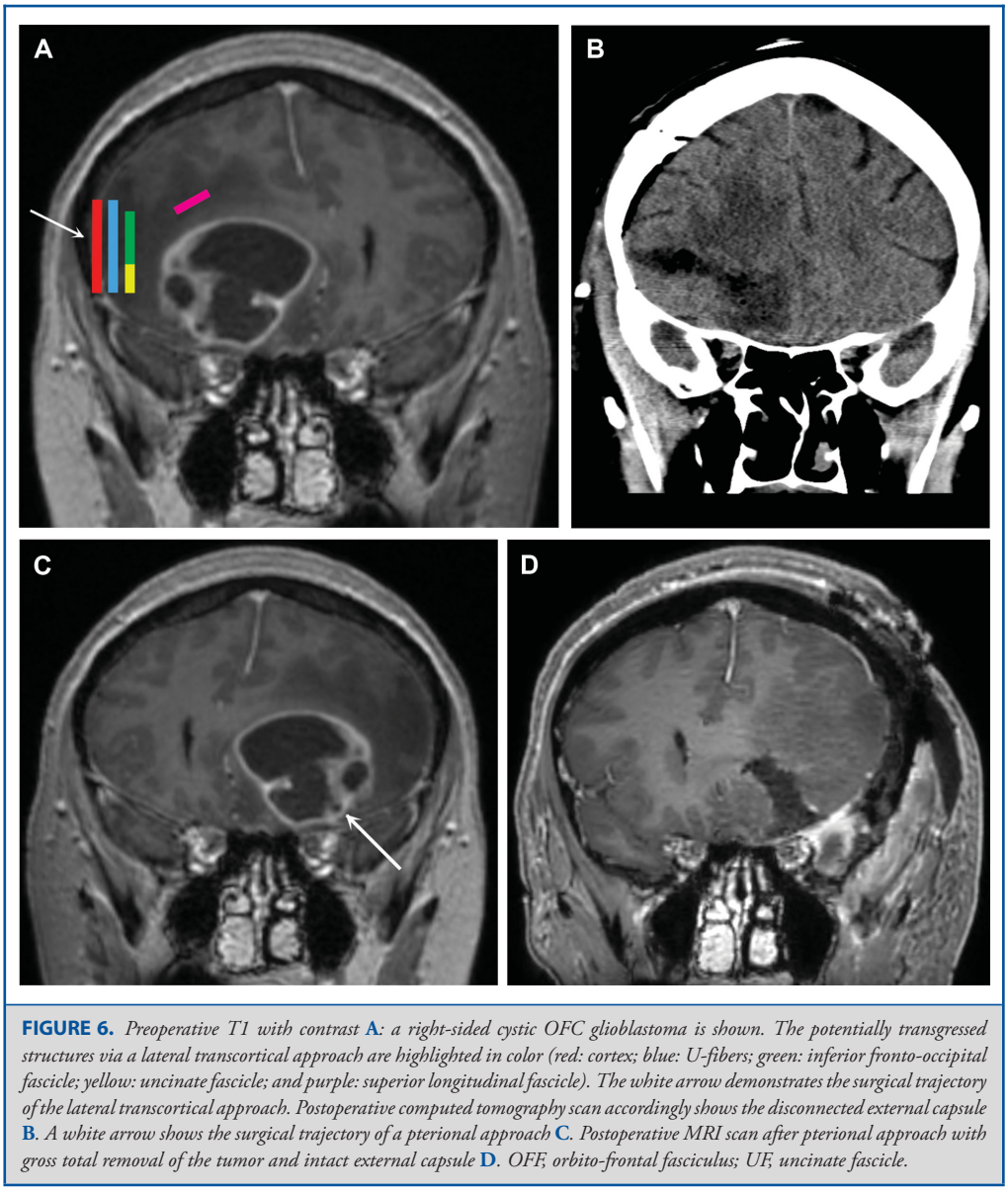

FIGURE 6. *Preoperative T1 with contrast* **A***: a right-sided cystic OFC glioblastoma is shown. The potentially transgressed structures via a lateral transcortical approach are highlighted in color (red: cortex; blue: U-fibers; green: inferior fronto-occipital fascicle; yellow: uncinate fascicle; and purple: superior longitudinal fascicle). The white arrow demonstrates the surgical trajectory of the lateral transcortical approach. Postoperative computed tomography scan accordingly shows the disconnected external capsule* **B***. A white arrow shows the surgical trajectory of a pterional approach* **C***. Postoperative MRI scan after pterional approach with gross total removal of the tumor and intact external capsule* **D***. OFF, orbito-frontal fasciculus; UF, uncinate fascicle.*

patients can play an effective role in the process of understanding the 3-dimensional and tissue-specific tumor characteristics that can otherwise easily be missed.

Surgical Implications

We favored a pterional approach for all of our patients to enable us to resect the tumor from an inferior orbitofrontal trajectory. Opening and careful microdissection of the opticocarotid and of the proximal sylvian cisterns allow for significant cerebrospinal fluid egress and a posterior relaxation of the frontal lobe. After identification of the optic nerve and of the internal carotid artery, the olfactory striae and olfactory nerve are identified as key posteromedial landmarks. The carotid bifurcation together with the M1 segment of the middle cerebral artery facilitates a reliable indirect identification of the APS as posterior-lateral resection border. Altogether, these steps enable the surgeon to approach the OFC directly from an inferior trajectory without the need for retractors. Moreover, and most importantly, they facilitate a selective tumorectomy within the OFC without the need of a lateral transcortical pathway or an anatomical disruption of otherwise healthy anatomical structures (ie, the laterally displaced external capsule or of the frontal neocortex). To anticipate displaced white and grey matter structures and to plan a nontraumatic operative trajectory

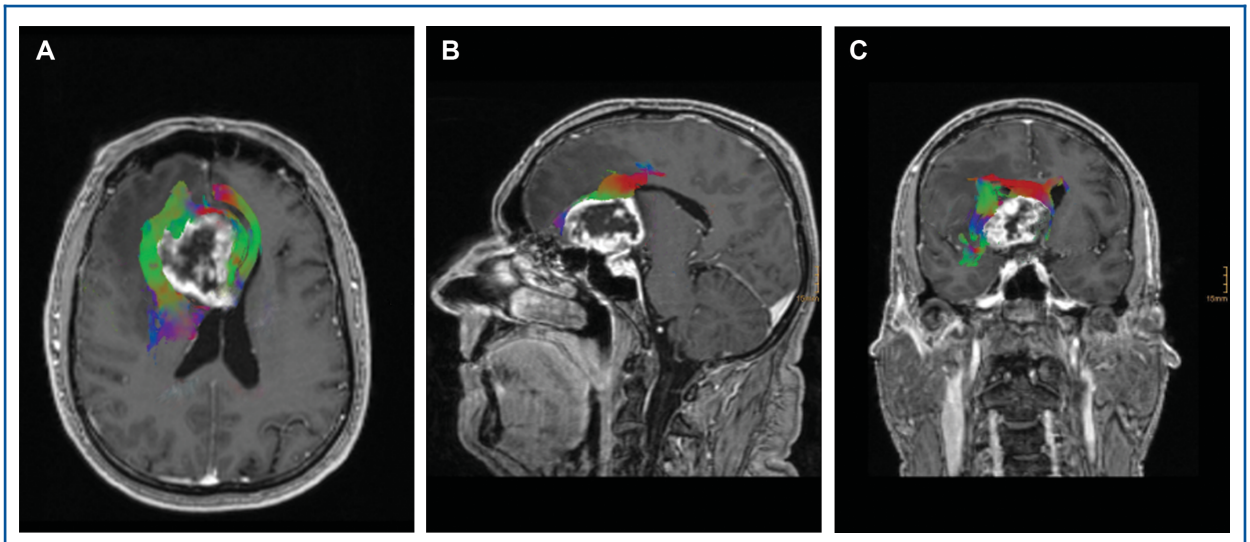

FIGURE 7. *Diffusion tensor imaging of an OFC glioma on a 3-Tesla MRI. Postprocessing via syngo, via software package (Siemens). From left to right:* **A**, *transversal,* **B**, *sagittal, and* **C**, *coronal view. Intact lateral fibers including the external capsule and frontopontine fibers of the internal capsule (green* **A** *and blue* **C**). *Note the displaced but intact corpus callosum (red) and its frontal extension of the forceps minor limiting the superior extension of the tumor* **B**.

accordingly, is of crucial importance for a beneficial onco-functional outcome.

To the best of our knowledge, this case series is the first study to show specific homologous glioma behavior in the OFC.

CONCLUSION

Neocortical structures of the frontal lobe are frequently affected in brain cancer patients. Our study highlights a specific growth pattern of glioma in the OFC. Detailed anatomical knowledge of the respective glioma site not only enables the surgeon to conduct the surgical removal effectively and safely but might also contribute to the understanding of key principles in glioma evolution.

Funding

This study did not receive any funding or financial support.

Disclosures

The authors have no personal, financial, or institutional interest in any of the drugs, materials, or devices described in this article.

REFERENCES

1. Mai JK, Paxinos G, Voss T. *Atlas of the Human Brain*. 3rd ed. Academic Press; 2007.
2. Damasio H, Grabowski T, Frank R, Galaburda AM, Damasio AR. The return of Phineas Gage: clues about the brain from the skull of a famous patient. *Science*. 1994;264(5162):1102-1105.
3. Nogueira R, Abolafia JM, Drugowitsch J, Balaguer-Ballester E, Sanchez-Vives MV, Moreno-Bote R. Lateral orbitofrontal cortex anticipates choices and integrates prior with current information. *Nat Commun*. 2017;8(1):14823.
4. Stalnaker TA, Cooch NK, Schoenbaum G. What the orbitofrontal cortex does not do. *Nat Neurosci*. 2015;18(5):620-627.
5. Duffau H, Capelle L. Preferential brain locations of low-grade gliomas. *Cancer*. 2004;100(12):2622-2626.
6. Ellingson BM, Lai A, Harris RJ, et al. Probabilistic radiographic atlas of glioblastoma phenotypes. *AJNR Am J Neuroradiol*. 2013;34(3):533-540.
7. Gilbertson RJ, Gutmann DH. Tumorigenesis in the brain: location, location, location. *Cancer Res*. 2007;67(12):5579-5582.
8. Cabrera S, Edelstein K, Mason WP, Tartaglia MC. Assessing behavioral syndromes in patients with brain tumors using the frontal systems behavior scale (FrSBe). *Neuro-Oncol Pract*. 2016;3(2):113-119.
9. Catani M, Dell'acqua F, Bizzi A, et al. Beyond cortical localization in clinico-anatomical correlation. *Cortex J Devoted Study Nerv Syst Behav*. 2012;48(10):1262-1287.
10. Duffau H. The "frontal syndrome" revisited: lessons from electrostimulation mapping studies. *Cortex*. 2012;48(1):120-131.
11. Taphoorn MJB, Klein M. Cognitive deficits in adult patients with brain tumours. *Lancet Neurol*. 2004;3(3):159-168.
12. Serra C, Türe U, Krayenbühl N, Şengül G, Yaşargil DCH, Yaşargil MG. Topographic classification of the thalamus surfaces related to microneurosurgery: a white matter fiber microdissection study. *World Neurosurg*. 2017;97(Jan):438-452.
13. Türe U, Yaşargil MG, Friedman AH, Al-Mefty O. Fiber dissection technique: lateral aspect of the brain. *Neurosurgery*. 2000;47(2):417-427; discussion 426-427.
14. Duvernoy HM, Cabanis E-A, Iba-Zizen M-T, Tamraz J, Guyot J. *Le Cerveau Humain: Surface, Coupes Sériées Tridimensionnelles et IRM*. Springer; 1992.
15. Mesulam M-M. *Principles of Behavioral and Cognitive Neurology*. 2nd ed. Oxford University Press; 2000.
16. Nieuwenhuys R, Voogd J, Huijzen C van. *The Human Central Nervous System: A Synopsis and Atlas*. 3rd ed. Springer-Verlag; 1988.
17. Petrides M, Pandya DN. Comparative cytoarchitectonic analysis of the human and the macaque ventrolateral prefrontal cortex and corticocortical connection patterns in the monkey. *Eur J Neurosci*. 2002;16(2):291-310.
18. Ono M, Kubik S, Abernathey CD. *Atlas of the Cerebral Sulci*. Thieme Medical Publishers; 1990.
19. Chiavaras MM, LeGoualher G, Evans A, Petrides M. Three-dimensional probabilistic atlas of the human orbitofrontal sulci in standardized stereotaxic space. *NeuroImage*. 2001;13(3):479-496.

20. Serra C, Akeret K, Maldaner N, et al. A white matter fiber microdissection study of the anterior perforated substance and the basal forebrain: a gateway to the basal ganglia? *Oper Neurosurg*. 2019;17(3):311-320.
21. Jenkins LM, Andrewes DG, Nicholas CL, et al. Emotional reactivity following surgery to the prefrontal cortex. *J Neuropsychol*. 2018;12(1):120-141.
22. Filimonoff IN. A rational subdivision of the cerebral cortex. *Arch Neurol Psychiatry*. 1947;58(3):296-311.
23. Yakovlev PI. Pathoarchitectonic studies of cerebral malformations. III. Arrhinencephalies (holotelencephalies). *J Neuropathol Exp Neurol*. 1959;18(1):22-55.
24. Yaşargil MG, von Ammon K, Cavazos E, Doczi T, Reeves JD, Roth P. Tumours of the limbic and paralimbic systems. *Acta Neurochir (Wien)*. 1992;118(1-2):40-52.
25. Yasargil MG, Adamson TE, Cravens GF, Johnson RJ, Lang A. *Microneurosurgery*, 4 Vols., Vol.4A, Thieme: CNS Tumors.
26. Scherer HJ. Structural development in gliomas. *Am J Cancer*. 1938;34(3):333-351.
27. Cuddapah VA, Robel S, Watkins S, Sontheimer H. A neurocentric perspective on glioma invasion. *Nat Rev Neurosci*. 2014;15(7):455-465.
28. Diao W, Tong X, Yang C, et al. Behaviors of glioblastoma cells in in vitro microenvironments. *Sci Rep*. 2019;9(1):85.
29. Gillespie S, Monje M. An active role for neurons in glioma progression: making sense of Scherer's structures. *Neuro-Oncol*. 2018;20(10):1292-1299.
30. Gozé C, Mansour L, Rigau V, Duffau H. Distinct IDH1/IDH2 mutation profiles in purely insular versus paralimbic WHO grade II gliomas. *J Neurosurg*. 2013;118(4):866-872.
31. Sanchez-Vega F, Mina M, Armenia J, et al. Oncogenic signaling pathways in The Cancer Genome Atlas. *Cell*. 2018;173(2):321-337.e10.e10.
32. Westphal M, Lamszus K. The neurobiology of gliomas: from cell biology to the development of therapeutic approaches. *Nat Rev Neurosci*. 2011;12(9):495-508.
33. Alfonso JCL, Talkenberger K, Seifert M, et al. The biology and mathematical modelling of glioma invasion: a review. *J R Soc Interface*. 2017;14(136):20170490.
34. Jacobs J, Rockne RC, Hawkins-Daarud AJ, et al. Improved model prediction of glioma growth utilizing tissue-specific boundary effects. *Math Biosci*. 2019;312(Jun):59-66.
35. Swanson KR, Alvord EC, Murray JD. A quantitative model for differential motility of gliomas in grey and white matter. *Cell Prolif*. 2000;33(5):317-329.
36. Swanson KR, Rockne RC, Claridge J, Chaplain MA, Alvord EC, Anderson ARA. Quantifying the role of angiogenesis in malignant progression of gliomas: in silico modeling integrates imaging and histology. *Cancer Res*. 2011;71(24):7366-7375.
37. Negi SK, Guda C. Global gene expression profiling of healthy human brain and its application in studying neurological disorders. *Sci Rep*. 2017;7(1):1-12.
38. Venkatesh HS, Morishita W, Geraghty AC, et al. Electrical and synaptic integration of glioma into neural circuits. *Nature*. 2019;573(7775):539-545.
39. Schramm J, Aliashkevich AF. Surgery for temporal mediobasal tumors: experience based on a series of 235 patients. *Neurosurgery*. 2007;60(2):285-295; discussion 294-295.
40. Manini I, Caponnetto F, Bartolini A, et al. Role of microenvironment in glioma invasion: what we learned from in vitro models. *Int J Mol Sci*. 2018;19(1):147.
41. Mughal AA, Zhang L, Fayzullin A, et al. Patterns of invasive growth in malignant gliomas—the hippocampus emerges as an invasion-spared brain region. *Neoplasia*. 2018;20(7):643-656.
42. Engwer C, Hillen T, Knappitsch M, Surulescu C. Glioma follow white matter tracts: a multiscale DTI-based model. *J Math Biol*. 2015;71(3):551-582.